The Microlensing Event MACHO-99-BLG-22/OGLE-1999-BUL-32: An Intermediate Mass Black Hole, or a Lens in the Bulge

D.P. Bennett[1], A.C. Becker[2], J.J. Calitz[3], B.R. Johnson[4], C. Laws[5], J.L. Quinn[1], S.H. Rhie[1], and W. Sutherland[6]

ABSTRACT

We present an re-analysis of the longest timescale gravitational microlensing event discovered to date: MACHO-99-BLG-22/OGLE-1999-BUL-32, which was discovered by both the MACHO and OGLE microlensing alert systems. Our analysis of this microlensing parallax event includes a likelihood analysis of the lens position based upon a standard model of the Galactic velocity distribution, and this implies that the lens could be a black hole of $\sim 100 M_\odot$ at a distance of a few hundred parsecs in the Galactic disk or a massive stellar remnant (black hole or neutron star) in the Galactic bulge. Our new analysis includes data from the MACHO, GMAN, and MPS collaborations in addition to the OGLE data used in a previous analysis by Mao et al (2002). The crucial feature that distinguishes our analysis from that of Mao et al is an accurate constraint on the direction of lens motion and an analysis of the implications of this direction.

1. Introduction

The abundance of long timescale microlensing events towards the Galactic bulge has remained a puzzle (Han & Gould 1996; Bennett et al. 2002) since shortly after the first systematic analyses of Galactic bulge microlensing events were reported (Udalski et al. 1994a; Alcock et al. 1997b). A long time scale event can be caused by a massive lens, a slow relative transverse velocity between the lens and source, or by large source star-lens and lens-observer separations. Thus, the excess of long timescale events could be caused by errors in our assumptions regarding the phase space distribution of the source stars or the lenses, or they could be caused by an unexpectedly large population of massive lenses. However, the phase space distribution of stellar mass objects in the Galactic disk and bulge is tightly constrained by observations, whereas little is known about the mass function of massive stellar remnants. Thus, it is possible that the excess of long timescale events is due to a population of black holes and neutron stars that is larger than expected.

This possibility has recently received observational support from the MACHO (Bennett et al. 2002) and OGLE (Mao et al. 2002) collaborations which have identified individual candidate black hole microlensing

[1]Department of Physics, University of Notre Dame, IN 46556
[2]Bell Laboratories, Lucent Technologies, 600 Mountain Avenue, Murray Hill, NJ 07974
[3]Physics Department, University of the Free State, Bloemfontein 9300, South Africa
[4]Tate Laboratory of Physics, University of Minnesota, Minneapolis, MN 55455
[5]Departments of Astronomy and Physics, University of Washington, Seattle, WA 98195
[6]Royal Observatory, Blackford Hill, Edinburgh EH9 3HJ

events based upon the detection of the microlensing parallax effect (Refsdal 1966; Gould 1992; Alcock et al. 1995). This refers to the detection of light curve features due to the Earth's accelerating motion around the Sun, and it is often detectable in long timescale microlensing events. To date, some 12 clear cases of this effect have been reported by the MACHO (Alcock et al. 1995; Bennett et al. 2002; Becker 2000), OGLE (Mao 1999; Soszyński et al. 2001; Smith, Mao, & Woźniak 2001; Mao et al. 2002), MOA (Bond et al. 2001) and PLANET (An et al. 2002) collaborations. These microlensing parallax events are useful because they allow one to learn more about the nature of the lens than can be learned for most microlensing events. For most microlensing events, the only measurable parameter which constrains interesting properties of the lens is the Einstein diameter crossing time, $\widehat{t}$, which depends on the lens mass (M), distance (D_ℓ), and the magnitude of the transverse velocity ($v_\perp = |\mathbf{v}_\perp|$). It is given by

$$\widehat{t} = \frac{2R_E}{v_\perp} = \frac{4}{v_\perp c}\sqrt{\frac{GMD_\ell(D_s - D_\ell)}{D_s}}\ , \tag{1}$$

where D_s refers to the distance to the source (typically $\sim 8\,$kpc for a bulge source), and R_E is the radius of the Einstein Ring. In a microlensing parallax event, it is also possible to measure $\tilde{v}$, which is the lens star's transverse speed projected to the Solar position, given by

$$\tilde{\mathbf{v}} = \mathbf{v}_\perp \mathbf{D_s}/(\mathbf{D_s} - \mathbf{D}_\ell)\ . \tag{2}$$

The measurement of both $\widehat{t}$ and $\tilde{v}$ give us two measurements for three unknowns (M, $v_\perp$, and D_ℓ), which allows us to solve for the mass as a function of distance:

$$M = \frac{\tilde{v}^2\widehat{t}^2c^2}{16G}\frac{D_s - D_\ell}{D_\ell D_s} = \frac{\tilde{v}^2\widehat{t}^2c^2}{16G}\frac{1-x}{xD_s}\ , \tag{3}$$

where $x = D_\ell/D_s$. For the MACHO-99-BLG-22/OGLE-1999-BUL-32 microlensing event, (Mao et al. 2002) have used Eq. 3 to argue that the lens mass is well above the measured mass of neutron stars ($\sim 1.4\mathrm{M}_\odot$) for plausible values of x.

Bennett et al. (2002) have also made use of the measured direction of the projected velocity, $\tilde{\mathbf{v}}$, in a likelihood analysis employing the velocity and density distributions of a standard Galactic model. This allows a likelihood estimate for the lens distance, x, which can be converted to an estimate of the lens mass using Eq. 3. This analysis has revealed two other candidate black hole lenses, MACHO-96-BLG-5 and MACHO-98-BLG-6, as well as several other events with possible neutron star lenses. In this paper, we add additional data to the analysis of the MACHO-99-BLG-22/OGLE-1999-BUL-32 microlensing event, and show that this results in tighter constraints on the microlensing parallax parameters. We then apply the likelihood analysis developed in Alcock et al. (1995) and Bennett et al. (2002) to estimate the likely distance and mass of the lens.

2. The Data Set and Previous Analysis

The MACHO-99-BLG-22/OGLE-1999-BUL-32 microlensing event was discovered and announced by the MACHO Alert system[1] (Alcock et al. 1996), and it was independently discovered by the OGLE early warning system (Udalski et al. 1994b) about two months later. Following the MACHO alert, this event was added to the observing schedule for the GMAN (Becker 2000) and MPS (Rhie et al. 1999) microlensing follow-up groups. MACHO and GMAN observations ended in 1999, while MPS and OGLE observations continued through 2000. Photometry from the images of this event is particularly challenging because of severe crowding within $\sim 1.5''$ of the source star. This makes it difficult for point spread function fitting, crowded field photometry programs such as DOPHOT (Schechter, Mateo, & Saha 1993), DAOPHOT/ALLFRAME (Stetson 1994), or SoDOPHOT (Bennett et al. 1993; Alcock et al. 1999) to obtain accurate photometry for this event. For the GMAN and MPS images, we were able to solve this difficulty by carefully selecting template images with sub-arc second seeing, but no such images are available for the MACHO data. There is a great deal of scatter in the MACHO-red data which appears to be inconsistent with the other data sets. A similar problem was seen in the MPS data, but it disappeared when the MPS data was reduced with a better seeing image as a template. This suggests that the photometric problem with the MACHO-red data is due to close neighbor stars that are not quite resolved in the MACHO-red template. The MACHO-blue data has much less scatter, and so we have decided to use only the MACHO-blue data in our analysis.

The data set presented in this paper consists of 609 MACHO-Blue band measurements,[2] 245 OGLE I-band measurements from their catalog of difference imaging measurements (Wozniak et al. 2001), 179 MPS R-band observations from the Mt. Stromlo 1.9m telescope, and 21 GMAN R-band observations from the CTIO 0.9m telescope. The MPS data are reduced using a slightly modified version of the MACHO photometry code, SoDOPHOT. The photometric errors reported by SoDOPHOT are modified by adding a 1.0% assumed systematic uncertainty in quadrature. The CTIO data were reduced with the ALLFRAME package (Stetson 1994), with the error estimates multiplied by a factor of 1.5 to account for systematic errors.

A microlensing parallax fit for this event was previously published by Mao et al. (2002). However, Mao et al. (2002) present their fit results in a coordinate system that is inconvenient for Galactic bulge microlensing events. The difficulty is that all geometrical quantities are projected into the ecliptic plane, rather than a plane perpendicular to the line of site to the lens that is used for most discussions of microlensing events. Since the ecliptic plane intersects the Galactic bulge, this projection can be very nearly singular for Galactic bulge events. Instead, if we project the Earth's motion in the ecliptic plane to the plane perpendicular to the line of site (as in Alcock et al. (1995), for example), then there is no singularity. Event MACHO-99-BLG-22/OGLE-1999-BUL-32 is about 5 degrees from the ecliptic plane ($\lambda = 271.122°$, $\beta = -5.142°$).

[1] A catalog of MACHO alert events is available at `http://darkstar.astro.washington.edu/` along with some information regarding each event. However, the reported timescales of these events are systematically underestimated because they come from fits that do not allow for blending.

[2] The MACHO Project survey data are available from `http://wwwmacho.mcmaster.ca/` and `http://wwwmacho.anu.edu.au`.

This means that the transformations of the error bars from the coordinate system of Mao et al. (2002) to our coordinate system are highly non-linear, and it means that the $1\,\sigma$ error bars reported in Mao et al. (2002) cannot be used to estimate the $2\,\sigma$ error bars. Because of this difficulty and the fact that Mao et al. (2002) use a data set which differs from the publicly available one, we will not attempt a detailed comparison of our fit parameters with their results.

3. Microlensing Parallax Analysis

The magnification for a normal microlensing event with no detectable microlensing parallax is given by

$$A(t) = \frac{u^2+2}{u\sqrt{u^2+4}}\ ;\ \ u(t) \equiv \sqrt{u_0^2 + [2(t-t_0)/\widehat{t})]^2}\ , \tag{4}$$

where t_0 is the time of closest approach between the angular positions of the source and lens, and $u_0 = b/R_E$ where b is the distance of the closest approach of the lens to the observer-source line. Eq. (4) can be generalized to the microlensing parallax case (Alcock et al. 1995) by assuming the perspective of an observer located at the Sun. We can then replace the expression for $u(t)$ with

$$\begin{aligned} u^2(t) \ &= \ u_0^2 + \omega^2(t-t_0)^2 + \alpha^2\sin^2[\Omega(t-t_c)] \\ &\quad +2\alpha\sin[\Omega(t-t_c)]\,[\omega(t-t_0)\sin\theta + u_0\cos\theta] \\ &\quad +\alpha^2\sin^2\beta\,\cos^2[\Omega(t-t_c)] + 2\alpha\sin\beta\,\cos[\Omega(t-t_c)]\,[\omega(t-t_0)\cos\theta - u_0\sin\theta] \end{aligned} \tag{5}$$

where λ and β are the ecliptic longitude and latitude, respectively, θ is the angle between $v_\perp$ and the North ecliptic axis, $\omega = 2/\widehat{t}$, and t_c is the time when the Earth is closest to the Sun-source line. The parameters α and Ω are given by

$$\alpha = \frac{\omega(1\mathrm{AU})}{\tilde{v}}\,(1-\epsilon\cos[\Omega_0(t-t_p)])\ , \tag{6}$$

and

$$\Omega(t-t_c) = \Omega_0(t-t_c) + 2\epsilon\sin[\Omega_0(t-t_p)]\ , \tag{7}$$

where t_p is the time of perihelion, $\Omega_0 = 2\pi\,\mathrm{yr}^{-1}$, $\epsilon = 0.017$ is the Earth's orbital eccentricity.

The microlensing parallax fits were performed with the MINUIT routine from the CERN Library, and the results are summarized in Table 1, and are shown in Fig. 1 The first four fit parameters listed in Table 1 are fit blend fractions for each of the four data sets. Because the OGLE data was reduced with a difference imaging method, there is no photometric reference flux value to use to define $f_{\mathrm{OGLE}} = 1$. Therefore, we select the fit flux for the best parallax fit to define $f_{\mathrm{OGLE}} = 1$.

Although the comparison with the parallax fit of (Mao et al. 2002) is complicated by their peculiar choice of coordinates, we can compare to their $\widehat{t}$ and $\tilde{v}$ values since these are not affected by their coordinate system. They find $\widehat{t} = 1280^{+140}_{-110}$ days and $\tilde{v} = 79 \pm 16$ km/s, while we find $\widehat{t} = 1120 \pm 90$ days and $\tilde{v} = 75^{+7}_{-9}$ km/s. We find that the parallax fit gives an overall χ^2 improvement of 541.7 which compares

to the χ^2 improvement of 298.1 found by (Mao et al. 2002). Thus, our results seem to be somewhat more accurate, but consistent with the Mao et al fit.

The microlensing parallax fit parameters can be used to determine the lens mass as a function of distance following Eq. 3 as shown in Fig. 2.

3.1. Likelihood Distance and Mass Estimates

We can make use of our knowledge of the phase space distribution of lens objects in the Galactic disk and bulge to further constrain the distance and mass of the lens because the probability to obtain the measured value of $\tilde{\mathbf{v}}$ is quite sensitive to the distance to the lens. Following Alcock et al. (1995) and Bennett et al. (2002), we can define a likelihood function

$$L(x;\tilde{\mathbf{v}}) \propto \sqrt{x(1-x)}\,\rho_L(x)\,\tilde{v}(1-x)^3 \int f_S(\mathbf{v}_S)\, f_L((1-x)(\mathbf{v}_\odot+\tilde{\mathbf{v}})+x\mathbf{v}_S)\, d\mathbf{v}_S, \tag{8}$$

where ρ_L is the density of lenses at distance $x = D_\ell/D_s$, and the integral is over combinations of source and lens velocities giving the observed $\tilde{\mathbf{v}}$. $\mathbf{v}_S$ and $\mathbf{v}_L = (1-x)(\mathbf{v}_\odot+\tilde{\mathbf{v}})+x\mathbf{v}_S$ are the 2-D source and lens velocity distribution functions. We assume the following Galactic parameters: a disk velocity dispersion of $30\,\mathrm{km/s}$ in each direction, a flat disk rotation curve of $200\,\mathrm{km/s}$, and a bulge velocity dispersion of $80\,\mathrm{km/s}$ with no bulge rotation. The density profiles are a standard double-exponential disk and a Han & Gould (1996) barred bulge, and the source star is assumed to reside the the Galactic bulge at a distance of $8.5\,$kpc which is consistent with the measured radial velocity, $v_r = +38 \pm 2\,$km/sec of the source star (Cook et al. 2002).

The resulting likelihood functions for D_ℓ is shown as the long-dashed curves in Fig. 2. This differs from the likelihood functions for the six events presented by Bennett et al. (2002) because it has two peaks. This is because the measured direction of $\tilde{\mathbf{v}}$ is nearly opposite of the direction of Galactic disk rotation. For a typical Galactic disk lens, we expect $\tilde{\mathbf{v}}$ to be roughly parallel to the disk rotation direction as is observed for the six MACHO events analyzed in Bennett et al. (2002). Since the bulge is assumed to have little or no rotation, the average line-of-site to a bulge lens is stationary at the position of the source. (A rotating bar-shaped bulge could imply an average bulk motion at along some lines-of-sight.) The flat rotation curve of the Galactic disk will cause stars orbiting interior to the Solar circle to have a higher angular velocity than the Sun, and so the preferred projected velocity, $\tilde{\mathbf{v}}$ will be in the direction of Galactic disk rotation. However, the probability for $\tilde{\mathbf{v}}$ to be in the anti-preferred direction is not small (Bennett et al. 2002), so the fit parameters for MACHO-99-BLG-22/OGLE-1999-BUL-32 should not be considered unlikely.

The double peaked nature of the likelihood function shown in Fig. 2 can easily be understood if we consider the ways in which a $\tilde{\mathbf{v}}$ parallel to the Galactic disk rotation can be avoided. One possibility is for a disk lens to be very close to us. In this case, the average Galactic angular velocity at the lens position is only slightly larger than that of the Sun, and so the velocity dispersion of the disk will give a substantial population of potential lens objects with retrograde $\tilde{\mathbf{v}}$ values. The other possibility is that the lens resides in the Galactic bulge where there is little or no systematic rotation. In this case, with both the lens and

source in the bulge, the Galactic orbital motion of the Sun gives a preference for a retrograde $\tilde{\mathbf{v}}$ value, but the preference is fairly small because the lens must be much closer to the source than to the Sun. The two likelihood function peaks can be then understood as being due to disk and bulge lenses. This is clear from the decomposition of the likelihood function shown in Fig. 2. For a disk lens, the likelihood function peaks at a mass of $130\mathrm{M}_\odot$, which is about an order of magnitude above the most massive of the known stellar mass black holes in x-ray binary systems. If the lens is in the bulge, however, the most likely mass is only about $4\mathrm{M}_\odot$.

One common way to interpret likelihood functions is the Bayesian method, in which the lens mass (or distance) probability distribution is given by the likelihood function times a prior distribution, which represents our prior knowledge of the probability distribution. In our case, the likelihood function represents all of our knowledge about the lens mass and location, so we select a uniform prior. With a uniform prior, the likelihood function becomes the probability distribution, and we are able to calculate the lens mass confidence levels listed in Table 2. Also included in this table are the lens mass confidence levels if the lens is known to be a disk or a bulge star. If the lens resides in the disk, Table 2 indicates that the lens mass should be in the range $16\mathrm{M}_\odot < \mathrm{M} < 172\mathrm{M}_\odot$ at $1\,\sigma$ and $6.3 < M < 900\mathrm{M}_\odot$ at $2\,\sigma$. This wide range is due to the fact that the distance to a disk lens is not well constrained. If the lens resides in the bulge, then the mass range is much narrower: $2.2\mathrm{M}_\odot < \mathrm{M} < 5.5\mathrm{M}_\odot$ at $1\,\sigma$ and $1.34\mathrm{M}_\odot < \mathrm{M} < 8.3\mathrm{M}_\odot$ at $2\,\sigma$. This suggests a low mass black hole, although a neutron star or even a main sequence lens cannot be ruled out.

3.2. Constraint on a Possible Main Sequence Lens

If the lens star is a main sequence star, then there is an additional constraint on the distance and mass of the lens due to the observed upper limit on the brightness of the lens star (Bennett et al. 2002). We have assigned a conservative upper limit on the V-band brightness of $V > 20.1 \pm 0.5$ based upon the best parallax fit. We have applied this constraint to the likelihood function by multiplying the likelihood function by the Gaussian probability that the lens brightness exceeds upper limit on the lens star brightness. The result is shown as the alternating short and long-dashed curve in Fig. 2, which indicates that main sequence lens stars more massive than about $1.5\mathrm{M}_\odot$ is ruled out. A much tighter constraint on the brightness of the lens can be obtained with HST images as has been done with the MACHO-96-BLG-5 black hole candidate (Bennett et al. 2002).

4. Discussion and Conclusions

We have presented a microlensing parallax analysis of the MACHO-99-BLG-22/OGLE-1999-BUL-32 microlensing event using the publicly available OGLE and MACHO data along with MPS and GMAN data. The projected velocity indicated by the microlensing parallax fit has a direction that is nearly opposite of the direction of disk rotation. This suggests that the lens is either very close to us in the Galactic disk or in the Galactic bulge. The microlensing parallax mass-distance relationship, 3, indicates that the lens must be

very massive if it is nearby, with a mass of order $\sim 100 M_\odot$. If the lens is in the Galactic bulge, however, its mass is much smaller, $\sim 4 M_\odot$. In both cases, the lens is likely to be a black hole. These conclusions have been quantified with a likelihood analysis similar to those presented by Alcock et al. (1995) and Bennett et al. (2002). We should note that this analysis does depend on the assumption that stellar mass black holes are not born with a large velocity "kick." This assumption is supported by the available evidence (Nelemans, Tauris, & van den Heuvel 1999), but if this assumption is wrong, then the MACHO-99-BLG-22/OGLE-1999-BUL-32 could be a $\sim 10 M_\odot$ black hole half way to the Galactic with a rotation speed of only about $60\,\mathrm{km/s}$.

We have not carried a Bayesian likelihood analysis with an assumed mass distribution prior as has been advocated by Agol et al. (2002) and also done by Bennett et al. (2002). Such an analysis is of little use for this event because the lens mass is very likely to be $> 1.5 M_\odot$. Since a main sequence lens of this mass is excluded, we would have to provide a prior distribution of stellar remnants, but there is virtually nothing known about mass function of stellar remnants above $1.5 M_\odot$.

Our analysis agrees with the previous analysis of Mao et al. (2002) and indicates that the MACHO-99-BLG-22/OGLE-1999-BUL-32 lens is very likely to be a black hole, but we show that a nearby, massive black hole of $\sim 100 M_\odot$ and a low mass black hole of $\sim 4 M_\odot$ in the Galactic bulge are two distinct possibilities that can explain the observed microlensing parallax parameters. When this event is combined with the two other candidate black hole microlenses presented by the MACHO Collaboration (Bennett et al. 2002), it appears that black holes may comprise a significant fraction of the mass of the Galactic disk and bulge, perhaps as large as $\sim 10\%$. Future observations with large ground based interferometers (Delplancke, Górski, & Richichi 2001) should be able to accurately determine the mass of future black hole microlenses and determine the black hole mass fraction.

This work was supported, in part, through the NASA Origins Program Grant NAG5-4573.

REFERENCES

Agol, E., et al. 2002, ApJ, submitted (astro-ph/0203257)

Alcock, C., et al. 1995, ApJ, 454, L125

Alcock, C., et al. 1996, ApJ, 463, L67

Alcock, C., et al. 1997b, ApJ, 479, 119; (E) 500, 522

Alcock, C., et al. 1999, PASP, 111, 1539

An, J., et al. 2002, ApJ, in press (astro-ph/0110095)

Becker, A. C. 2000, PhD thesis, University of Washington

Bennett, D. P. et al. 1993, American Astronomical Society Meeting, 183, 7206

Bennett, D. P., et al. 2002, ApJ, in press (astro-ph/0109467)

Bond, I., et al. 2001, MNRAS, 327, 868.

Cook, K., et al. 2002, in preparation

Delplancke, F., Górski, K. M., & Richichi, A. 2001, A&A, 375, 701

Gould, A. 1992, ApJ, 392, 442

Han, C. & Gould, A. 1996, ApJ, 467, 540

Mao, S. 1999, A&A, 350, L19

Mao, S. et al. 2002, MNRAS, 329, 349

Nelemans, G., Tauris, T. M., & van den Heuvel, E. P. J. 1999, A&A, 352, L87.

Refsdal, S. 1966, MNRAS, 134, 315

Rhie, S. H., Becker, A. C., Bennett, D. P., Fragile, P. C., Johnson, B. R., King, L. J., Peterson, B. A., & Quinn, J. 1999, ApJ, 522, 1037

Schechter, P. L., Mateo, M., & Saha, A. 1993, PASP, 105, 1342

Smith, M. C., Mao, S., & Woźniak, P. 2001, MNRAS, submitted.

Soszyński, I. et al. 2001, ApJ, 552, 731

Stetson, P. B. 1994, PASP, 106, 250

Udalski, A. et al. 1994a, Acta Astronomica, 44, 165

Udalski, A., Szymański, M., Kałużny, J., Kubiak, M., Mateo, M., Krzmiński, W., & Paczyński , B. 1994b, Acta Astronomica, 44, 227

Wozniak, P. R., Udalski, A., Szymanski, M., Kubiak, M., Pietrzynski, G., Soszynski, I., & Zebrun, K. 2001, Acta Astronomica, 51, 175.

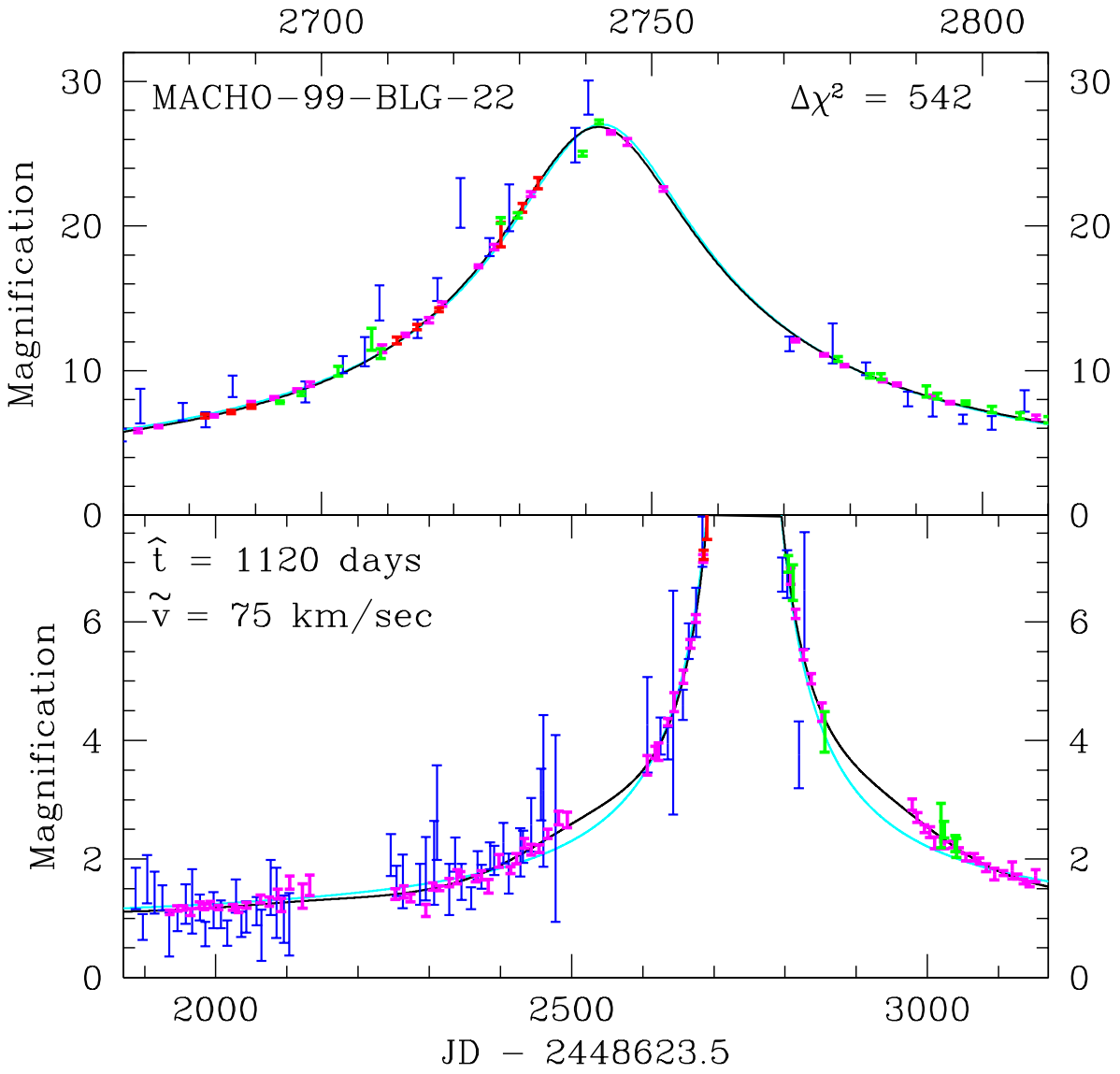

Fig. 1.— The light curve of the MACHO-99-BLG-22/OGLE-1999-BUL-32 microlensing event with data from MACHO, OGLE, MPS and GMAN. The blue, green, red, and magenta data points indicate data from the MACHO-Blue band, the Mt. Stromlo 1.9m R-band,the CTIO 0.9m R-band, and the OGLE I-band, respectively. The solid curve shows the best fit microlensing parallax event while the cyan curve shows the best fit standard microlensing light curve. In the upper panel, the data have been averaged into 4-day bins, while in the lower panel the data have been averaged into 10-day bins.

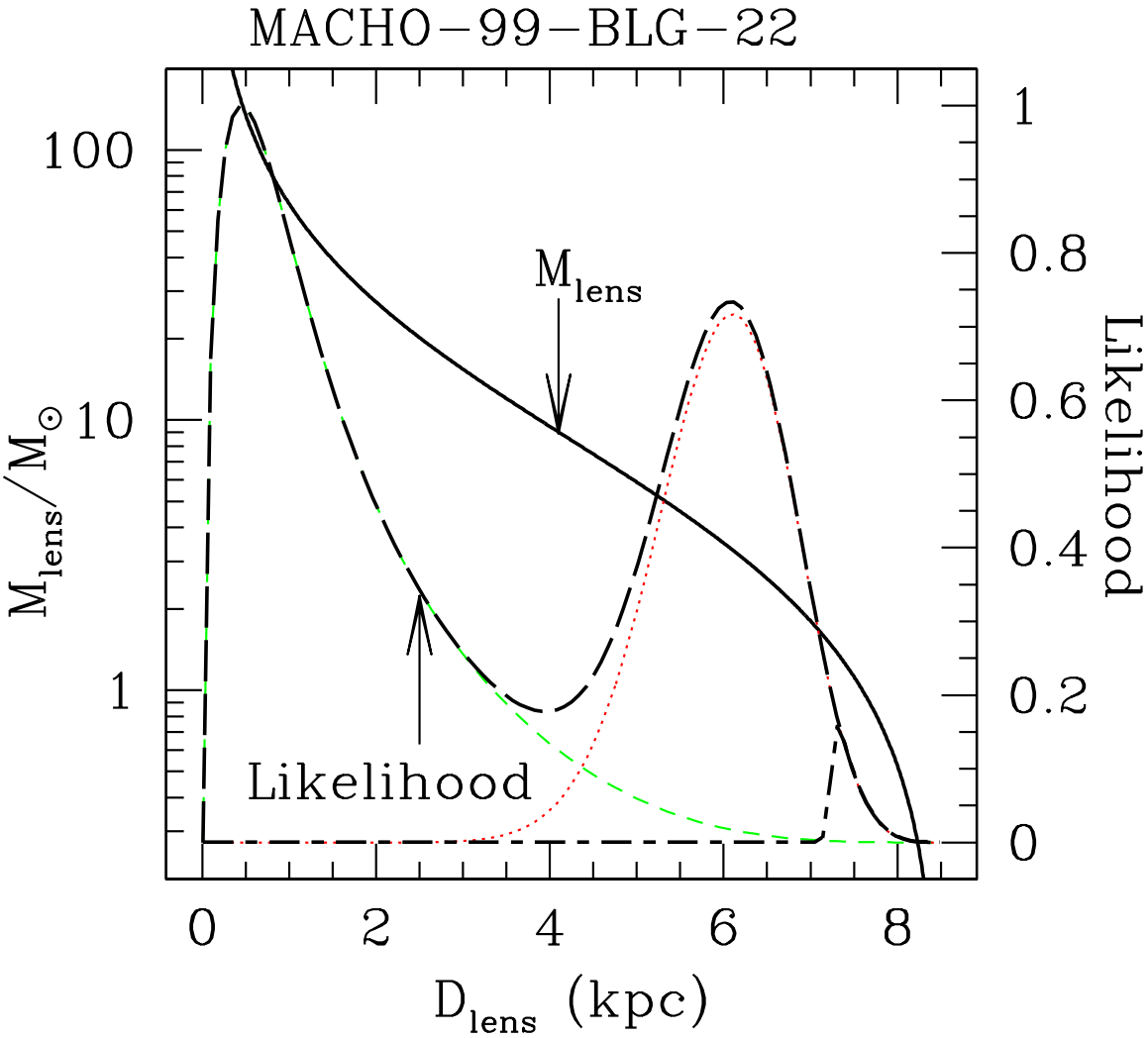

Fig. 2.— The mass vs. distance relation (solid curves) for the MACHO-99-BLG-22/OGLE-1999-BUL-32 microlensing event is shown along with the likelihood functions (long dashed curves) computed assuming a standard model for the Galactic phase space distribution. The (green) short dashed curve is the contribution from disk lenses, and the (red) dotted curve is the contribution from bulge lenses. The alternating long and short dashed curve is the likelihood function which includes the constraint on the brightness of a main sequence lens star. A main sequence lens is quite unlikely for this event.

Table 1. Microlensing Fit Parameters

Fit	$f_{\rm OGLE}$	$f_{\rm MB}$	$f_{\rm CTIO}$	$f_{\rm MPS}$	t_0 (MJD)	u_0	$\widehat{t}$ (days)	$\tilde{v}$ (km/sec)	θ	$\frac{\chi}{(\mathrm{d}}$
Par.	$1.00(11)$	$0.26(3)$	$0.44(5)$	$0.46(5)$	$2745.0(1.5)$	$0.043(6)$	$1120(90)$	$75(9)$	$1.85(20)$	0.8
Std.	$0.02(5)$	$0.005(3)$	$0.01(1)$	$0.01(1)$	$2742.4(1)$	$0.0007(1)$	$4.0(2) \times 10^4$	$\equiv 0$	$\equiv 0$	1.3

Table 2. Microlensing Parallax Likelihood Mass Estimates

	Confidence Levels $P(M/\mathrm{M}_\odot < \mathrm{N})$						
lens location	$P = 2.5\%$	$P = 5\%$	$P = 16\%$	$P = 50\%$	$P = 84\%$	$P = 95\%$	$P = 97.5\%$
disk or bulge	560	310	106	17.1	3.2	2.1	1.70
disk	900	480	172	49	16.2	8.5	6.3
bulge	8.3	7.3	5.5	3.6	2.2	1.60	1.34